

Superfluid Suppression in d -Wave Superconductors due to Disordered Magnetism

W. A. Atkinson

Trent University, 1600 West Bank Dr., Peterborough ON, K9J 7B8, Canada

(Dated: September 10, 2018)

The influence of static magnetic correlations on the temperature-dependent superfluid density $\rho_s(T)$ is calculated for d -wave superconductors. In self-consistent calculations, itinerant holes form incommensurate spin density waves (SDW) which coexist with superconductivity. In the clean limit, the density of states is gapped, and $\rho_s(T \ll T_c)$ is exponentially activated. In inhomogeneously-doped cases, the SDW are disordered and both the density of states and $\rho_s(T)$ obtain forms indistinguishable from those in dirty but pure d -wave superconductors, in accordance with experiments. We conclude that the observed collapse of ρ_s at $x \approx 0.35$ in underdoped $\text{YBa}_2\text{Cu}_3\text{O}_{6+x}$ may plausibly be attributed to the coexistence of SDW and superconductivity.

I. INTRODUCTION

High temperature superconductors (HTS) are an ideal class of materials with which to study electronic correlations in superconductivity because the correlations can be tuned from weak to strong via chemical doping. A consequence of strong-correlation physics is that the BCS theory of conventional superconductors fails to describe HTS. Uemura demonstrated that, unlike in BCS theory where the superfluid density ρ_s and critical temperature T_c are independent, HTS exhibit an approximate scaling $\rho_s \propto T_c^1$. The physical origin of the Uemura relation is not known conclusively but is consistent with strong-correlation models^{2,3,4} in which the quasiparticle spectral weight, and consequently ρ_s , are proportional to the hole concentration p , where p is measured relative to the Mott insulator phase. However, these models fail to explain both the collapse of superconductivity at a nonzero doping $p_c \approx 0.05$ and the breakdown of the Uemura relation near p_c , shown by recent experiments in $\text{YBa}_2\text{Cu}_3\text{O}_{6+x}$ (YBCO)^{5,6}.

A number of authors^{7,8} have suggested that T_c is governed by phase fluctuations, possibly in combination with quasiparticle excitations⁹, and in particular that the rapid collapse of ρ_s and T_c at p_c can be thus explained¹⁰. In this work, we examine a completely different mechanism: the suppression of superfluidity by the formation of static magnetic moments. This is motivated by a substantial body of experimental evidence for the presence of quasistatic magnetism in underdoped HTS.^{11,12,13,14,15,16,17,18,19} There have been previous suggestions that some form of competing order is important in the underdoped HTS,^{20,21,22,23} and in particular there have been numerous studies of the competition between d -wave superconductivity and commensurate antiferromagnetism.^{24,25,26,27,28} These are generally difficult to reconcile with superfluid density measurements largely because the competing order introduces an identifiable energy scale. Calculations show that this energy scale appears in the temperature dependence of the superfluid density^{29,30,31} but such an energy scale has not been observed experimentally³¹. Indeed, recent microwave conductivity measurements⁶ of the superfluid

depletion, $\delta\rho_s(T) \equiv \rho_s(0) - \rho_s(T)$, in high quality single crystals of YBCO find $\delta\rho_s(T) \propto T$ with a crossover to $\delta\rho_s(T) \propto T^2$ when $T \ll T_c$. The linear T -dependence is expected in a single-phase d -wave superconductor and the low- T crossover to T^2 behavior has been attributed to residual impurity scattering. It is therefore not *a priori* clear that the experimentally observed magnetic moments have any significant effect on the electronic spectrum. Here, we show that a phase of coexisting spin density wave (SDW) and d -wave superconducting (dSC) order can, provided the SDW is disordered, have a spectrum indistinguishable from that of a dirty dSC. We conclude that the rapid collapse of superfluid density near p_c could indeed be due to magnetism.

Our approach is semi-phenomenological. We construct a mean-field model in which the model parameters are assumed to have been dressed by electron interactions. The approach is motivated by a variety of calculations,^{2,3,24,32,33,34} mostly for the t - J model, in which mean-field theories are developed for which the parameters are functions of p . In the simplest Gutzwiller approximation for the t - J model,³⁴ for example, the renormalized kinetic energy operator \hat{T} is related to the bare kinetic energy operator \hat{T}_0 by $\hat{T} = \hat{T}_0 2p/(1+p)$. Other results are found in other approximations,^{2,3,24,32,33} but all show the same qualitative result that \hat{T} is reduced as one approaches the Mott insulating phase. In dynamical mean-field theory calculations, this derives from a self-energy which renormalizes both the quasiparticle spectral weight and effective mass.³⁵ We remark that the effective interactions are also expected to depend on the doping, generally increasing as p is reduced. This is ignored in our calculations since it will have a quantitative but not qualitative effect on the outcome. The essential physics in the current discussion is that, near the magnetic phase boundary a small change in the mean-field parameters produces a much larger change in the magnetic state. The progression from pure dSC to pure magnetic order depends only on the general trend that the ratio of kinetic to interaction energies decreases as p decreases.

In section II we introduce the model and describe the phase diagram. The most significant result of this section is that it is possible to have substantial *incommensurate*

magnetic moments coexist with the superconductivity, with very little suppression of the pair amplitude. This is in contrast with the more widely studied case of *commensurate* magnetic order, which suppresses superconductivity rapidly.^{24,25,26,27,28} In section III, we calculate both the density of states and the superfluid density for the incommensurate phases. As mentioned previously, we find the surprising result that when the magnetic moments are disordered, the spectrum is indistinguishable from that of a dirty *d*-wave superconductor. We conclude briefly in section IV.

II. MODEL AND PHASE DIAGRAM

The HTS consist of conducting two-dimensional CuO₂ layers that are weakly coupled along the perpendicular direction. We model the lower Hubbard band of a single two-dimensional layer with an extended Hubbard model, treated at a mean-field level. Our numerical calculations have found that the results are only weakly dependent on the filling p but depend sensitively on the quasiparticle bandwidth and Fermi surface curvature. As discussed above, we assume that doping effects occur indirectly through a parameter $w(p)$ which renormalizes the quasiparticle dispersion. For simplicity, and since the detailed relationship between w and p is not established, we will treat w as the independent parameter, and keep all other parameters fixed.

Calculations are for an N -site two-dimensional tight-binding lattice with periodic boundary conditions and lattice constant $a_0 = 1$, similar to one used previously to study the local density of states in underdoped HTS³⁶. The Hamiltonian is

$$\hat{H}_H = w \sum_{ij\sigma} t_{ij} c_{i\sigma}^\dagger c_{j\sigma} + U \sum_{i\sigma} \hat{n}_{i\sigma} n_{i\bar{\sigma}} + \sum_{\langle i,j \rangle} \Delta_{ij} (\hat{f}_{ij} + \hat{f}_{ij}^\dagger) \quad (1)$$

where t_{ij} are the hopping matrix elements of the tight-binding band, i and j are site-indices, σ is the electron spin, and $\bar{\sigma} \equiv -\sigma$. We take $t_{ij} = t_0$ for $i = j$ and $t_{ij} = t_n$, $n = 1, \dots, 3$, for n th nearest-neighbor sites i and j . Taking $\{t_0, \dots, t_3\} = \{1.7, -1, 0.45, -0.1\}$ gives the Fermi surface shown in Fig. 1. The local electronic density $n_{i\sigma} \equiv \langle \hat{n}_{i\sigma} \rangle$, where $\hat{n}_{i\sigma} = c_{i\sigma}^\dagger c_{i\sigma}$, is determined self-consistently and the hole density is $p_{i\sigma} = 1 - n_{i\sigma}$. The magnetic order parameter is then $m_i = (n_{i\uparrow} - n_{i\downarrow})/2$, and the staggered moment is $m_i^Q = (-1)^{x_i+y_i} m_i$ where $\mathbf{r}_i = (x_i, y_i)$ is the coordinate of site i . The nearest neighbor pairing term $\Delta_{ij} = -\frac{J}{2} \langle \hat{f}_{ij} \rangle$, with $\hat{f}_{ij} = (c_{j\downarrow} c_{i\uparrow} - c_{j\uparrow} c_{i\downarrow})/2$ is also determined self-consistently and has pure dSC symmetry, $\Delta_{ij} = \frac{\Delta}{4} (-1)^{y_j - y_i}$, in the nonmagnetic phase.

To allow for inhomogeneous doping we add dopant-impurity and Coulomb interaction terms, also treated at the mean-field level:

$$\hat{H}_c = \sum_{i \neq j} V(\mathbf{r}_i - \mathbf{r}_j) \hat{n}_i n_j - Z \sum_i \sum_{\ell=1}^{N_I} V(\mathbf{r}_i - \mathbf{R}_\ell) \hat{n}_i, \quad (2)$$

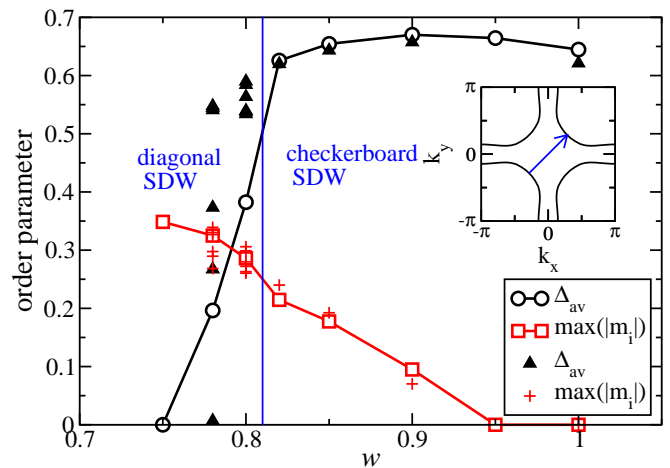


FIG. 1: (Color online) Phase diagram as a function of kinetic energy renormalization. Open symbols are for the homogeneously doped calculations, closed triangle and + symbol are for inhomogeneously doped calculations. Inset: Fermi surface and CSDW nesting vector.

with $n_i = \sum_{\sigma} n_{i\sigma}$, Z the impurity charge, \mathbf{R}_ℓ the locations of the N_I impurities, and $V(\mathbf{r}) = e^2 e^{-r/\Lambda} / \epsilon a_0$ a weakly-screened Coulomb interaction, with $e^2 / \epsilon a_0 = 1.5$ and $\Lambda = 20a_0$. In the cuprate HTS, donor impurities typically sit a few Å above the CuO₂ layers, so we randomly choose values of $\mathbf{R}_\ell = (x_\ell, y_\ell, d)$ with $d = a_0$. The total hole doping is $p = ZN_I/N$. We study a homogeneously doped case with $N_I = N$ and $Z = p$, and an inhomogeneously doped case at the same filling with $N_I = N/4$ and $Z = 4p$. The resulting impurity potential is smoother than one expects in many underdoped HTS but is reasonable for underdoped YBCO where approximately 35% of chain oxygen sites are filled. It is assumed that strong-correlation renormalizations of V , J and U are included implicitly and remain constant over the narrow doping range explored here; for a given p , we choose J and U such that $w = 1$ corresponds to a pure dSC phase close to the magnetic phase boundary. We then follow the magnetic phase diagram, Fig. 1, as w is reduced. The results depend sensitively on the Fermi surface shape (ie. on t_2 and t_3), but depend only weakly on p which is therefore chosen for computational convenience. We have studied the parameter sets $(p, U, J) = (0.05, 3.4, 1.8)$ and $(p, U, J) = (0.35, 3.2, 1.5)$. The two agree semiquantitatively where we have been able to compare; however, it is difficult to obtain converged solutions for $p = 0.05$ when w is small, and we have chosen to present results for $p = 0.35$ where a full set of results is available.

The calculations proceed as follows. The Hamiltonian, written $\hat{H} = \mathbf{c}^\dagger \mathbf{H} \mathbf{c}$ with $\mathbf{c}^\dagger = [c_{1\uparrow}^\dagger \dots c_{N\uparrow}^\dagger c_{1\downarrow} \dots c_{N\downarrow}]$ and \mathbf{H} a Hermitian matrix, is diagonalized numerically giving the unitary matrix \mathbf{U} of eigenvectors and eigenvalues E_n .

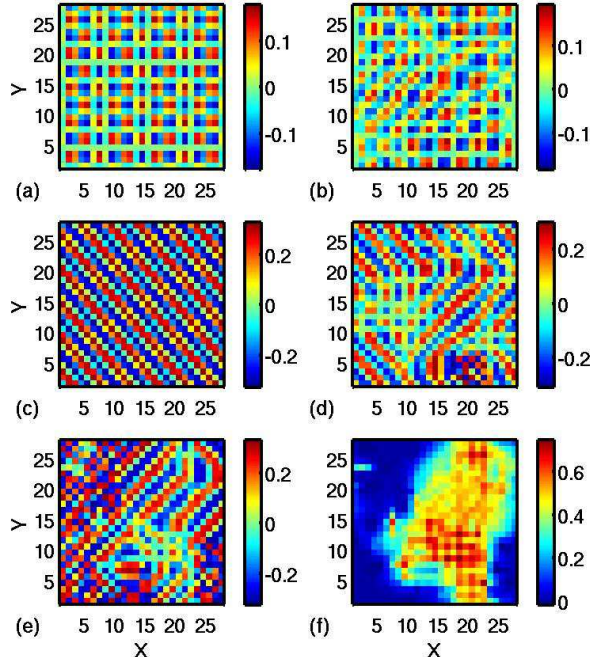


FIG. 2: (Color online) Typical self-consistent solutions. The staggered magnetization is shown for the CSDW phase at $w = 0.85$ (a,b) and the DSDW phase at $w = 0.8$ (c,d) with homogeneous (a,c) and inhomogeneous (b,d) doping; The magnetization (e) and dSC gap (f) are shown for $w = 0.78$ with inhomogeneous doping. Inhomogeneous results are for a single dopant configuration.

The calculations

$$n_{i\uparrow} = \sum_{n, E_n < 0} |U_{in}|^2 \quad (3)$$

$$n_{i\downarrow} = 1 - \sum_{n, E_n < 0} |U_{i+Nn}|^2 \quad (4)$$

$$\Delta_{ij} = -(J/2) \sum_{n, E_n < 0} (U_{in}U_{j+Nn} + U_{i+Nn}U_{jn}) \quad (5)$$

are iterated until the largest difference between successive values of Δ_{ij} and $n_{i\sigma}$ is less than 10^{-4} . At convergence, the total energy is typically varying in the tenth significant figure. Convergence is difficult to obtain: first, the charge density oscillates wildly in simple-iteration schemes because of the Coulomb interaction and, second, the magnetic moment configuration may fail to converge because the energy near self-consistency depends only weakly on it. A significant effort has been made to address both these issues. First, we have generated our initial guess for the local charge density using a self-consistent Thomas-Fermi calculation. In order not to bias the outcome of the calculation we have used 8-16 randomly seeded initial magnetic moment configurations for each parameter set, from which the lowest

energy self-consistent solution is retained. Second, we have adopted a Thomas-Fermi-Pulay iteration scheme,³⁷ which controls the iteration instability in most cases. Results shown here have all converged.

The phase diagram is shown in Fig. 1. For large w , there is a pure dSC phase. As w is reduced, there is a second order transition into a coexisting phase of dSC and checkerboard SDW (CSDW) order at $w \approx 0.95$, followed by a first order transition into a phase of coexisting dSC and diagonal SDW (DSDW) order at $w \approx 0.81$; both phases are illustrated in Fig. 2. Superconductivity is destroyed at $w \approx 0.76$. From Fig. 2, one sees that doping-induced inhomogeneity disorders the SDW and has a significant effect on the phase diagram in the dSC+DSDW phase: a typical solution for $w = 0.78$, shown in Fig. 2 (e,f), consists of an inhomogeneous mixture of pure SDW and dSC+SDW order, with superconductivity preferentially forming in hole-rich regions. The spatially-averaged Δ varies considerably between dopant configurations, as seen in Fig. 1, but within superconducting domains, the local order parameter is consistently $|\Delta_{ij}| \sim 0.5$; the destruction of superconductivity occurs inhomogeneously.

We can understand the origin of magnetic order in the CSDW phase; the Fourier transform $m(\mathbf{q})$ of m_i has a set of four peaks at $(\pi \pm \delta, \pi \pm \delta)$ and the inset to Fig. 1 shows that the vector $(\pi - \delta, \pi - \delta)$ taken from the data in Fig. 2(a) connects nodal points on the Fermi surface³⁸. The CSDW, therefore, nests portions of the Fermi surface where the pairing energy is small, and consequently minimizes competition between magnetic and dSC order. This explains why Δ is roughly constant throughout the dSC+CSDW phase (c.f. Fig. 1), and why the transition to the dSC+DSDW phase appears to occur only when the magnetic energy scale $M \approx U \max(|m_i|)$ is greater than Δ . It appears, then, as if CSDW ordering is stabilized by superconductivity. An analysis of $m(\mathbf{q})$ for the DSDW, in contrast, does not reveal any nesting of high-symmetry points, and Δ collapses rapidly in the dSC+DSDW phase.

These results are in striking contrast to what one finds for the case of commensurate magnetic order. We show, in Fig. 3 the results of calculations for the antiferromagnetic moment m_z and the dSC order parameter Δ determined self-consistently in the homogeneous limit. The calculation proceeds as follows: Adopting a four-component notation²⁶ $\mathbf{A}_{\mathbf{k}} \equiv (c_{\mathbf{k}\uparrow}, c_{-\mathbf{k}\downarrow}^\dagger, c_{\mathbf{k}+\mathbf{Q}\uparrow}, c_{-\mathbf{k}-\mathbf{Q}\downarrow}^\dagger)^T$ where $c_{\mathbf{k}\sigma} = N_k^{-1/2} \sum_i c_{i\sigma} \exp(-i\mathbf{k} \cdot \mathbf{r}_i)$, one can write $H = \sum_{\mathbf{k}} \mathbf{A}_{\mathbf{k}}^\dagger \mathbf{H}_{\mathbf{k}} \mathbf{A}_{\mathbf{k}}$ where the prime indicates a sum over $k_x > 0$ and

$$\mathbf{H}_{\mathbf{k}} = \begin{bmatrix} \epsilon_{\mathbf{k}} & \Delta_{\mathbf{k}} & -M & 0 \\ \Delta_{\mathbf{k}} & -\epsilon_{\mathbf{k}} & 0 & -M \\ -M & 0 & \epsilon_{\mathbf{k}+\mathbf{Q}} & \Delta_{\mathbf{k}+\mathbf{Q}} \\ 0 & -M & \Delta_{\mathbf{k}+\mathbf{Q}} & -\epsilon_{\mathbf{k}+\mathbf{Q}} \end{bmatrix}, \quad (6)$$

with the band energy $\epsilon_{\mathbf{k}} = t_0 + 2t_1(\cos k_x + \cos k_y) + 4t_2 \cos k_x \cos k_y$ and $\Delta_{\mathbf{k}} = \frac{\Delta}{2}(\cos k_x - \cos k_y)$ and $M =$

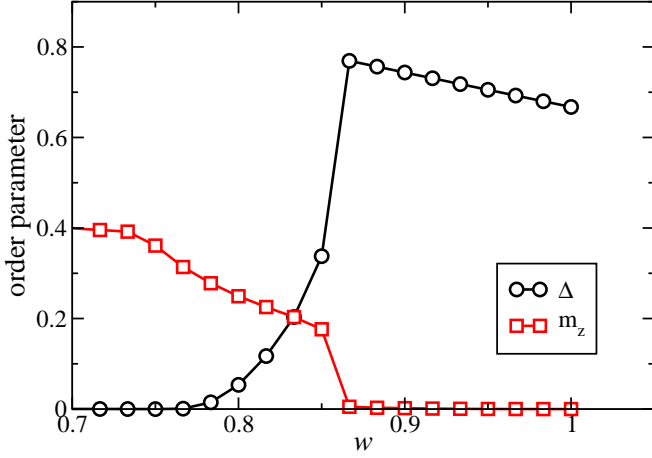


FIG. 3: (Color online) Phase diagram for commensurate order. Here, $U = 3.6$ while other parameters are as given in the text.

Um_z . If the 4×4 matrix diagonalizing $\mathbf{H}_{\mathbf{k}}$ is denoted $\mathbf{U}_{\mathbf{k}}$, then the self-consistent equations for Δ and m_z are

$$\Delta = -\frac{J}{N_k} \sum_{j=1}^4 \sum_{\substack{\mathbf{k}, \\ E_{j\mathbf{k}} < 0}} (\cos k_x - \cos k_y) U_{1j\mathbf{k}} U_{2j\mathbf{k}}, \quad (7)$$

$$m_z = \frac{1}{2N_k} \sum_{j=1}^4 \sum_{\substack{\mathbf{k}, \\ E_{j\mathbf{k}} < 0}} [U_{1j\mathbf{k}} U_{3j\mathbf{k}} + U_{2j\mathbf{k}} U_{4j\mathbf{k}}]. \quad (8)$$

Figure 3 shows that the dSC and antiferromagnetic order parameters are generally incompatible, with only a small coexistence region. More extensive studies of the phase diagram with commensurate order by Kyung²⁶ show that the size of the coexistence region depends on the model parameters, but that the antiferromagnetic and dSC order always suppress one another. By contrast, the CSDW order has very little effect on the dSC phase.

III. DENSITY OF STATES AND SUPERFLUID DENSITY

Because of the nodal nesting, the density of states (DOS)

$$N(\omega) = \sum_{i=1}^N \sum_{n=1}^{2n} [|U_{in}|^2 \delta(\omega - E_n) + |U_{i+Nn}|^2 \delta(\omega + E_n)], \quad (9)$$

develops a gap of width δ in the dSC+CSDW phase, as shown in Fig. 4. In contrast, the dSC+DSDW phase retains the characteristic d -wave DOS, $N(\omega) \propto |\omega|$ at low ω , but develops a resonance at ω_0 which in many cases dominates the spectrum. In both cases, these qualitative differences from the pure dSC DOS are reflected in $\rho_s(T)$.

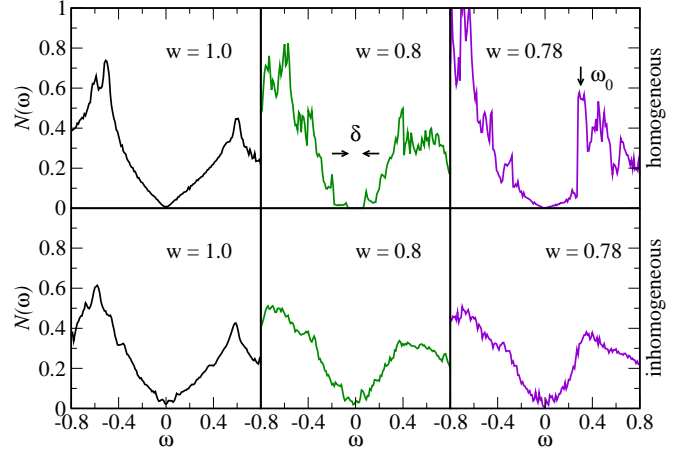


FIG. 4: (Color online) Density of states. $N(\omega)$ is shown for homogeneous (top row) and inhomogeneous (bottom row) doping. Inhomogeneous results are for a single dopant configuration, except for $w = 0.78$ which is averaged over 5 configurations. The single-particle gap δ and subgap resonance at ω_0 are indicated.

The superfluid density is related to the magnetic penetration depth $\lambda(T)$ measured in experiments by $\rho_s(T) = mc^2/4\pi e^2 \lambda^2(T)$. In linear-response theory, $\lambda^{-2}(T) = (4\pi e^2/c^2) \langle K_{\alpha\alpha}^{\text{dia}}(T) - K_{\alpha\alpha}^{\text{param}}(T) \rangle_{\alpha=x,y}$ with

$$K_{\alpha\beta}^{\text{dia}} = \sum_m [\tilde{M}_{\alpha\beta}^{-1}]_{mm} f(E_m) \quad (10)$$

$$K_{\alpha\beta}^{\text{para}} = \sum_{m,n} [\tilde{\gamma}_{\alpha}]_{mn} [\tilde{\gamma}_{\beta}]_{nm} \frac{f(E_m) - f(E_n)}{E_m - E_n} \quad (11)$$

where

$$[\tilde{\mathbf{M}}^{-1}]_{mn} = \sum_{i,j} \sum_{p=0}^1 (-1)^p U_{m i+pN}^{\dagger} [\mathbf{M}^{-1}]_{ij} U_{j+pN} n$$

$$[\tilde{\gamma}]_{mn} = \sum_{i,j} \sum_{p=0}^1 U_{m i+pN}^{\dagger} [\gamma^{-1}]_{ij} U_{j+pN} n$$

where $\tilde{\mathbf{M}}$ and $\tilde{\gamma}$ are the inverse effective mass tensor and current vertex respectively, written in the basis of eigenstates of the Hamiltonian. On a tight-binding lattice, $[M_{\alpha\beta}^{-1}]_{ij} = -t_{ij} \vec{\alpha} \cdot \mathbf{r}_{ij} \mathbf{r}_{ij} \cdot \vec{\beta}$ and $[\gamma_{\alpha}]_{ij} = i \vec{\alpha} \cdot \mathbf{r}_{ij} t_{ij}$ with $\vec{\alpha}$ and $\vec{\beta}$ the unit vectors \hat{x} or \hat{y} and $\mathbf{r}_{ij} = \mathbf{r}_i - \mathbf{r}_j$. The calculations are restricted to low T where we can use the $T = 0$ values for Δ_{ij} and $n_{i\sigma}$; the T -dependence of $\rho_s(T)$ is due to thermal pair breaking, as has been argued in Ref. [2]. We discuss this assumption below.

We focus first on homogeneous doping, Fig. 5(a). The superfluid density at $T = 0$ is a strong function of w , especially in the dSC+DSDW phase; $\rho_s(0)$ is reduced to 10% of its initial value with only small changes in the coherence peak energy in the DOS. While this is consistent with experiments, the T -dependence of $\rho_s(T)$ is

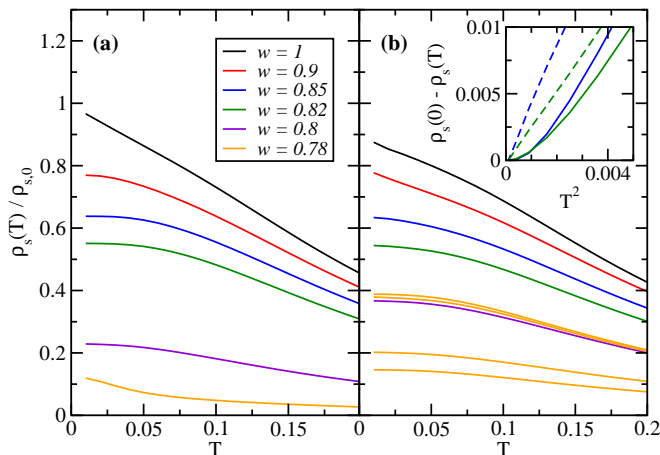


FIG. 5: (Color online) Superfluid density. $\rho_s(T)$ is plotted for homogeneous (a) and inhomogeneous (b) doping. Different curves for $w = 0.78$ in (b) correspond to different randomly-generated impurity potentials. Inset: low- T behavior of $\rho_s(T)$ for homogeneous (solid) and inhomogeneous (dashed) doping. Results in (b) are configuration-averaged over 2-4 samples, except for $w = 0.78$ where results are shown for each configuration.

not. In the dSC+CSDW phase, $\rho_s(T)$ is exponentially activated: $\delta\rho_s(T) \propto \exp(-T/\delta)$, where δ is the single-particle gap shown in Fig. 4. In the dSC+DSDW phase, $\rho_s(T)$ is linear in T , but also has an exponential contribution from the resonance at ω_0 , also shown in Fig. 4. In most cases we have studied the exponential contribution is dominant.

The inhomogeneously-doped calculations are qualitatively different. The electronic potential produced by doping is itself weakly scattering and has little direct effect on nodal quasiparticles³⁹; however, it disorders the SDW, and indirectly does have a significant effect on the low- ω DOS. As seen in Fig. 4, characteristic features of the different SDW phases are washed out and $N(\omega)$ universally obtains a dirty- d -wave form. This is one of the main results of this work. Not surprisingly, $\rho_s(T)$ also obtains the dirty dSC form; as shown in Fig. 5(b) and in the figure inset, $\delta\rho_s(T) \propto T^2$ for $T \ll T_c$, and is linear in T at larger T . In general, $\rho_s(T)$ varies weakly between disorder configurations. The notable exception is near the superconducting phase boundary (ie. $w = 0.78$) where $\rho_s(0)$ depends strongly on disorder configuration, although $\delta\rho_s(T)$ remains quadratic in T . In macroscopic samples, this will be reflected as a sensitivity to both sample quality and doping. The remarkable aspect of Fig. 5(b) is that, even for a magnetic energy scale $M \sim 2\Delta$ (at which point $\rho_s(0)$ is near zero), $\rho_s(T)$ has the appearance of a dirty but pure dSC, as seen in experiments. This constitutes our main finding.

The mechanism by which the superfluid density is depleted is quite interesting. The diamagnetic response, K^{dia} , is almost independent of both w and the magnetic

moment: however, the paramagnetic response at $T = 0$, $K^{\text{para}}(0)$, is a strong function of the magnetic moment. This is reminiscent of the response to disorder in d -wave superconductors where Cooper pair breaking by impurity scattering manifests as a nonzero $K^{\text{para}}(0)$. In this case, however, the broken Cooper pairs are also apparent as a finite residual density of states at the Fermi level. A disorder level sufficient to cause a 90% reduction in $\rho_s(0)$, as we have found here, would produce a residual density of states comparable to that of the normal state. The fact that such a residual density of states is *not* observed in our case illustrates that the SDW correlations are not simply breaking Cooper pairs.

Rather, it is the fact that Cooper pairs in the magnetic phase do not have a well-defined charge-current which is responsible for the suppression of $\rho_s(0)$. In the commensurate (four-band) case, the current operator is

$$\gamma_x(\mathbf{k}) = \begin{bmatrix} v_x(\mathbf{k})\tau_0 & 0 \\ 0 & v_x(\mathbf{k} + \mathbf{Q})\tau_0 \end{bmatrix} \quad (12)$$

with $v_x = \partial\epsilon_{\mathbf{k}}/\partial k_x$ and τ_0 the Pauli matrix. This matrix is not diagonal in the basis of Bogoliubov quasiparticles (ie. $\tilde{\gamma}_x(\mathbf{k})$ is not diagonal), meaning that the current is not conserved. Physically, this is because the Bogoliubov quasiparticles are formed from mixtures of states with crystal momenta \mathbf{k} and $\mathbf{k} + \mathbf{Q}$. Then, because $\tilde{\gamma}_x(\mathbf{k})$ has nonzero off-diagonal matrix elements, there is a nonzero interband contribution in Eq. (11) which reduces the overall superfluid density. We stress that this mechanism is distinct from either pair-breaking or quasiparticle renormalization (ie. strong-correlation) mechanisms for reducing the superfluid density.

We finish with a comment on the relationship between T_c and $\rho_s(0)$. An estimate of T_c as the temperature at which a straight line, fitted to the region $T > 0.1$ in Fig. 5(b), crosses the T -axis yields $T_c \approx 0.36$, for all w . This is surprising, as it indicates that even for strongly inhomogeneous cases T_c is determined by the maximum, rather than average, Δ . It also suggests that two physical processes neglected in our calculations, phase fluctuations and glassy SDW dynamics, may play an important role at higher T . In particular, phase fluctuations are expected to be pronounced at small w where the superconductivity is spatially inhomogeneous. Glassy spin dynamics, provided they remain slow on electronic time scales, behave as quenched disordering of the SDW, and should not change our results qualitatively. An interesting question, outside the scope of this work, is how the SDW dynamics affect $\rho_s(T)$ at higher doping, where a gap in the spin-wave spectrum begins to appear. In summary, it seems likely that, as suggested in Ref.⁹, T_c is ultimately determined by a combination of phase and quasiparticle excitations.

IV. CONCLUSIONS

In conclusion, we have shown that incommensurate magnetic correlations which nest the nodal points of the Fermi surface may coexist with d -wave superconductivity with essentially no suppression of the superconducting order. Furthermore, the formation of quasistatic moments is a plausible explanation for the rapid suppression of superfluid density near p_c in YBCO. We find that, provided the spin density waves are disordered, both the single-particle spectrum and $\rho_s(T)$ are indistinguishable

from the dirty d -wave case.

ACKNOWLEDGMENTS

This work was performed with the support of Research Corporation grant CC6062, of NSERC of Canada, and of the Canadian Foundation for Innovation. We acknowledge helpful conversations with R. J. Gooding, M. Randeria, N. Trivedi and Y. Song.

-
- ¹ Y. J. Uemura *et al.*, Phys. Rev. Lett. **62** 2317 (1989).
² Patrick A. Lee and Xiao-Gang Wen, Phys. Rev. Lett. **78** 4111 (1997).
³ Arun Paramekanti, Mohit Randeria, and Nandini Trivedi, Phys. Rev. B **70**, 054504 (2004).
⁴ P. W. Anderson, P. A. Lee, M. Randeria, T. M. Rice, N. Trivedi, and F. C. Zhang, J. Phys. Condens. Matter **16**, 755 (2004).
⁵ Yuri Zuev, Mun Seog Kim, and Thomas R. Lemberger, Phys. Rev. Lett. **95**, 137002 (2005).
⁶ D. M. Broun, P. J. Turner, W. A. Huttema, S. Ozcan, B. Morgan, Ruixing Liang, W. N. Hardy, and D. A. Bonn, cond-mat/0509223.
⁷ V. J. Emery and S. A. Kivelson, Nature **374**, 434 (1995).
⁸ E. Roddick and D. Stroud, Physica C **235**, 3696 (1995).
⁹ I. F. Herbut and M. J. Case, Phys. Rev. B **70**, 094516 (2004).
¹⁰ M. Franz and A. P. Iyengar, Phys. Rev. Lett. **96**, 047007 (2006).
¹¹ Ch. Niedermayer, C. Bernhard, T. Blasius, A. Golnik, A. Moodenbaugh, and J. I. Budnick, Phys. Rev. Lett. **80**, 3843 (1998).
¹² Y. Sidis, C. Ulrich, P. Bourges, C. Bernhard, C. Niedermayer, L. P. Regnault, N. H. Andersen, and B. Keimer, Phys. Rev. Lett. **86**, 4100 (2001).
¹³ H. A. Mook, Pengcheng Dai, S. M. Hayden, A. Hiess, J. W. Lynn, S.-H. Lee, and F. Doğan, Phys. Rev. B **66** 144513 (2002).
¹⁴ S. Sanna, G. Allodi, G. Concas, A. D. Hillier, and R. De Renzi, Phys. Rev. Lett. **93**, 207001 (2004).
¹⁵ B. Lake, H. M. Rnnow, N. B. Christensen, G. Aeppli, K. Lefmann, D. F. McMorrow, P. Vorderwisch, P. Smeibidl, N. Mangkorntong, T. Sasagawa, M. Nohara, H. Takagi and T. E. Mason, Nature **415**, 299 (2002); B. Lake, K. Lefmann, N. B. Christensen, G. Aeppli, D. F. McMorrow, H. M. Ronnow, P. Vorderwisch, P. Smeibidl, N. Mangkorntong, T. Sasagawa, M. Nohara, and H. Takagi, Nature Materials **4**, 658 (2005).
¹⁶ C. Panagopoulos, J. L. Tallon, B. D. Rainford, J. R. Cooper, C. A. Scott, and T. Xiang, Solid State Commun. **126**, 47 (2003); C. Panagopoulos and A. P. Petrovic and A. D. Hillier and J. L. Tallon and C. A. Scott and B. D. Rainford, Phys. Rev. B **69**, 144510 (2004).
¹⁷ J. A. Hodges and Y. Sidis and P. Bourges and I. Mirebeau and M. Hennion and X. Chaud, Phys. Rev. B **66**, 020501(R) (2002).
¹⁸ C. Stock, W. J. L. Buyers, Z. Yamani, C. L. Broholm, J.-H. Chung, Z. Tun, R. Liang, D. Bonn, W. N. Hardy, and R. J. Birgeneau, Phys. Rev. B **73**, 100504(R) (2006).
¹⁹ R. I. Miller, R. F. Kiefl, J. H. Brewer, F. D. Callaghan, J. E. Sonier, R. Liang, D. A. Bonn, and W. Hardy, Phys. Rev. B **73**, 144509 (2006).
²⁰ C. M. Varma, Phys. Rev. Lett. **83**, 3538 (1999).
²¹ S. Chakravarty, R. B. Laughlin, D. K. Morr, and C. Nayak, Phys. Rev. B **63**, 094503 (2001).
²² S. C. Zhang, Science 1089 (1997).
²³ G. Alvarez, M. Mayr, A. Moreo, and E. Dagotto, Phys. Rev. B **71**, 014514 (2005).
²⁴ M. Inui, S. Doniach, P. J. Hirschfeld, and A. E. Ruckenstein, Phys. Rev. B **37**, 2320 (1988).
²⁵ M. Murakami and H. Fukuyama, J. Phys. Soc. Jpn. **67**, 2784 (1998).
²⁶ Bumsoo Kyung, Phys. Rev. B **62** 9083 (2000).
²⁷ H. Yamase and H. Kohno, Phys. Rev. B **69**, 104526 (2004).
²⁸ J. Reiss, D. Rhohe, and W. Metzner, cond-mat/0611164.
²⁹ K.-K Voo and W. C. Wu Physica C **417**, 103-109 (2005)
³⁰ B. Tobijasewska and R. Micnas, Phys. Stat. Sol. **242**, 468 (2005).
³¹ Jelena Stajic, Andrew Iyengar, K. Levin, B. R. Boyce, and T. R. Lemberger, Phys. Rev. B **68**, 024520 (2003).
³² Gabriel Kotliar and Jialin Liu, Phys. Rev. B **38**, 5142(R) (1988).
³³ Yoshikazu Suzumura, Yasumasa Hasegawa, and Hidetoshi Fukuyama, J. Phys. Soc. Jap. **57** 2768 (1988).
³⁴ F. C. Zhang, C. Gros, T. M. Rice, and H. Shiba, Supercond. Sci. Technol., **1**, 36 (1988).
³⁵ Antoine Georges, Gabriel Kotliar, Werner Krauth, and Marcelo J. Rozenberg, Rev. Mod. Phys. **68**, 13 (1996).
³⁶ W. A. Atkinson, Phys. Rev. B **71**, 024516 (2005).
³⁷ D. Raczkowski, A. Canning, and L. W. Wang, Phys. Rev. B **64**, 121101(R) (2001).
³⁸ In k -space, the dSC order parameter is $\Delta_{\mathbf{k}} = \Delta(\cos k_x - \cos k_y)/2$, the nodal points are the points on the Fermi surface where $\Delta_{\mathbf{k}} = 0$. The antinodal points lie at the intersection of the Fermi surface and the zone boundary, where the gap obtains its maximum along the Fermi surface.
³⁹ T. S. Nunner, B. M. Andersen, A. Melikyan, and P. J. Hirschfeld, Phys. Rev. Lett. **95**, 177003 (2005).